

Transport behavior of water confined in carbon nanotubes

Yingchun Liu and Qi Wang*

Department of Chemistry, Zhejiang University, Hangzhou 310027, People's Republic of China

(Received 17 May 2005; published 5 August 2005)

The transport properties of water confined in single-walled carbon nanotubes with diameters from 1.1 nm to 2.1 nm were investigated by molecular dynamics simulations. It was found that the transport properties are anisotropic, the axial diffusivity, thermal conductivity, and viscosity are much larger than those in the radial direction. The diffusivity in carbon nanotubes is obviously lower than that of the bulk and it decreases as the diameter of the nanotube decreases. Particularly contrary to the diffusivity, the axial thermal conductivity and shear viscosity in carbon nanotubes is much higher than those of the bulk, and it increases sharply as the diameter of the nanotube decreases. The water molecules ordered in helix inside the (10, 10) single-walled carbon nanotube (SWCN) and the layered distribution was clearly observed.

DOI: [10.1103/PhysRevB.72.085420](https://doi.org/10.1103/PhysRevB.72.085420)

PACS number(s): 66.10.Cb, 66.20.+d, 66.60.+a, 81.07.De

The transport of simple and complex fluids in carbon nanotubes is important from both the fundamental science and the application points of view.¹⁻³ As we know, the liquid water is attractive for its anomalies in both the thermodynamic and the transport properties. The behavior of water inside single-walled carbon nanotubes (SWCNs) is of great interest for a number of reasons. Basically, a fundamental understanding of liquid flow and heat flow in nanochannels is still lacking. In addition, SWCNs may be used as nanometer-sized pipes in microfluidic systems, so control of liquid transport through SWCN is needed to develop such functional devices.^{1,4} It may also be useful as components in biosensors, minute chemical reactors, and drug delivery. Also, there are some discussions in the literature regarding the diffusion of simple fluids and simple alkanes.^{5,6} However in fact, besides the diffusivity, the transport properties also include the thermal conductivity and the viscosity. On the other hand, although there have been many studies on SWCNs, the main objectives of these studies are only focused in the properties of SWCNs themselves. The properties of the fluids confined in the SWCNs, for example, the transport properties and the molecular distribution, are poorly understood. Recently, the behaviors of water confined in a thin SWCN have been investigated. For example, Hummer,⁷ Zhou,⁸ and Maibaum⁹ presented a simple one-dimensional lattice gas model, which describes the equilibrium and kinetic behaviors of water confined in a thin SWCN. Rossi *et al.*¹⁰ studied the condensation, evaporation, and transport of water in SWCN. Fernandez *et al.*¹¹ reported the viscosity and the thermal conductivity of bulk simple fluids. However, the research works on the transport properties of complex fluids confined in nanogeometries, especially the thermal conductivity and the viscosity, and the development of these properties with the pore size, are rarely reported in the literature so far.

The diffusivity of confined water and argon in model nanopores has been extensively investigated in the previous works.¹²⁻¹⁶ For a more comprehensive study, the nanopore model used in the previous works was replaced with a more actual model nanopore, SWCN, and the other two transport properties of water, the thermal conductivity and the shear viscosity, were further explored in this work. The effects of

tube diameter on the transport behaviors and molecular distribution of water confined within SWCN were studied by molecular dynamics (MD) simulation.

The simple point charge (SPC) model¹⁷ for water was used in the MD simulations, whose intermolecular potential energy is given by the short-range Lennard-Jones potential between the interaction sites and by the Ewald summation of the long-range Coulombic potential. The force field of SWCNs was taken to be a Lennard-Jones form with the energy and size parameters for a carbon atom taken from graphite,¹⁸ $\epsilon_{ww}/k_B=28.0$ K and $\sigma_{ww}=0.34$ nm. The total interaction potential between water molecules and the confining wall of SWCN is calculated by using the site-site interaction method,

$$U_{fw} = 4\epsilon_{fw} \sum_{i=1}^{N_f} \sum_{j=1}^{N_{carbon}} \left[\left(\frac{\sigma_{fw}}{r_{ij}} \right)^{12} - \left(\frac{\sigma_{fw}}{r_{ij}} \right)^6 \right], \quad (1)$$

where N_f is the total number of atoms for water molecules, N_{carbon} is the total number of carbon atoms at the wall, and r_{ij} is the center-to-center distance between an atom of the water molecule and a carbon atom from the tubular wall. The subscript f denotes the fluid, and w denotes the wall. The cross energy and size parameters, ϵ_{fw} and σ_{fw} , are obtained from Lorentz-Berthlot combining rules,

$$\epsilon_{fw} = \sqrt{\epsilon_{ff} \times \epsilon_{ww}}, \quad (2)$$

$$\sigma_{fw} = (\sigma_{ff} + \sigma_{ww})/2. \quad (3)$$

The "armchair" (R,R) SWCNs with indices $R=8,10,12,14,16$, corresponding to the tube diameters of 1.08, 1.35, 1.55, 1.73, and 2.12 nm, respectively, were used in this work, and the atoms of SWCN wall were not allowed to move during the MD simulations. In the constant (number-of-molecules)-volume-temperature (NVT) ensemble, the MD time steps were performed by a modification of the TINKER package,¹⁹ which has been tested against the results available in the literature and used in the previous simulations.¹²⁻¹⁶ The periodic boundary condition was applied in the axial direction of the SWCNs to simulate the macroscopic systems. The cutoff distance of the potential function was taken to be 0.9

nm, and the time step was set to be 1 fs. The Beeman algorithm for integration of the equations of motion was employed in the MD time steps. In the simulations, the equilibration was verified primarily from the stability of the density profile and by whether the fluctuating of temperature was maintained within 0.2%. The first runs of 0.6×10^6 time steps (0.6 ns) were performed to relax and equilibrate the systems. Then, four runs of 1.2×10^6 time steps (1.2 ns) were used to analyze the statistical properties. The diffusivity (D), the thermal conductivity (λ), and the shear viscosity (η) of water were calculated from the Einstein expression for the diffusivity and from the Green-Kubo formula for the thermal conductivity and the viscosity.²⁰ The final results of D , λ , and η were obtained by averaging over all the four runs.²¹

$$D = \lim_{t \rightarrow \infty} \frac{1}{2td} \langle |r(t) - r(0)|^2 \rangle, \quad (4)$$

$$\lambda = \frac{1}{k_B T^2 V} \int_0^\infty \langle S(t)S(0) \rangle dt, \quad (5)$$

$$\eta = \frac{1}{k_B T V} \int_0^\infty \langle J_v(t)J_v(0) \rangle dt, \quad (6)$$

where $r(t)$ is the position of the center of mass of water molecules at time t , d is the degree of dimensions, k_B is the Boltzmann constant, T is the temperature, V is the volume of the simulation box, S is the heat flux, and J_v is the momentum flux.

Among transport properties, self-diffusion coefficients of fluids inside SWCNs have been more extensively studied^{5,6,22,23} than the thermal conductivity and the viscosity. For instance, based on MD and grand canonical Monte Carlo (GCMC) simulation, Cao *et al.*²⁴ investigated diffusivities of methane in SWCN. It was found that at low pressure, the diffusion coefficient of methane increases with the diameters of nanotubes. Despite a long history of research, many aspects of the transport phenomena in porous materials remain poorly understood.²⁵ The difficulties and challenges are that conventional transport theories are most adequate for describing macroscopic phenomena while the dynamics of molecules in small pores is often strongly affected by the interactions between fluid molecules and the confining walls, which leads to the situation becoming even more complicated. Based on the model nanopores used previously, the purpose of this work is focused to pay further attention to the transport properties of polar fluid, water, in actual SWCN. Figure 1 demonstrates that the diffusivity develops with the diameters of SWCNs at 298 K and 1.0 g cm^{-3} . The calculated axial diffusion coefficient is $D=0.9423 \times 10^{-9} \text{ m}^2 \text{ s}^{-1}$ in the (14, 14) SWCN, which well agrees with the result of Koga *et al.*²⁶ $D=1.0 \times 10^{-9} \text{ m}^2 \text{ s}^{-1}$ in the (14, 14) SWCN at 300 K but at 50 MPa. It is also observed that the diffusivity in SWCNs is much lower than that of the bulk, and it ever decreases as the diameter of SWCN decreases, which qualitatively agrees with the prediction of the Knudsen flow²⁷ and the diffusion model for the fluids confined in micropores,¹⁶ and it is similar to the results for the model nanopores re-

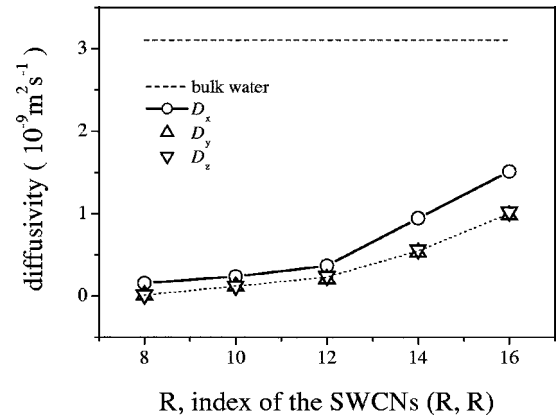


FIG. 1. The diffusivity and its components of water inside the SWCNs as a function of diameter of nanotubes at 298 K, 1.0 g cm^{-3} .

ported in our previous work. But the difference for these two types of nanopores is that the diffusivities in SWCNs are much less than that in model nanopores because of the interaction between the water molecules and the wall of the nanotubes.

As reported, the carbon nanotubes have a good thermal transport property.^{28,29} But how is the water confined in SWCNs? The variation of thermal conductivity of the confined water (the contribution of the SWCN itself was not included) along with the diameters of SWCNs is shown in Fig. 2. The thermal conductivity of water is anisotropic inside SWCNs whereas it is isotropic in the bulk. In contrast to the diffusivity, the axial thermal conductivity in nanotubes is much higher than that of the bulk, and it increases sharply as the diameter of SWCN decreases, but the radial thermal conductivity in nanotubes is much lower than the axial one. It can be explained by the fact that the pore space constrained causes the collision frequency of water molecules to be higher than that in the bulk and it increases as the diameter of SWCN decreases. Increases in collision frequency enhanced energy and heat transfer, so it leads to an increase in

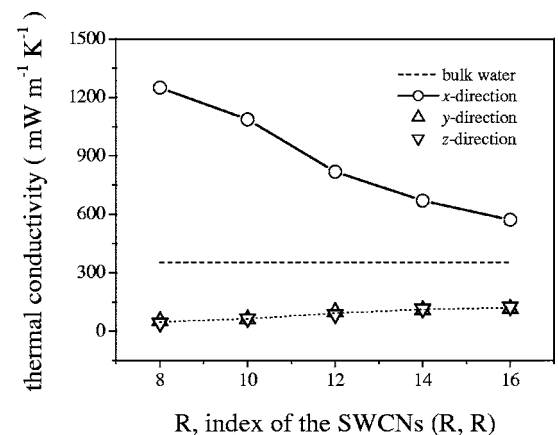


FIG. 2. The thermal conductivity and its components of water inside the SWCNs (the contribution of the SWCN itself was not included) as a function of diameter of nanotubes at 298 K, 1.0 g cm^{-3} .

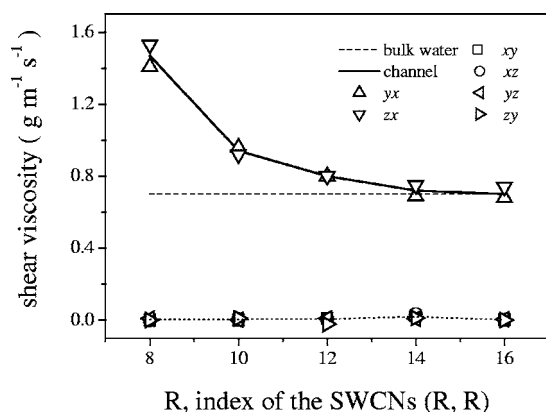


FIG. 3. The shear viscosity and its components of water inside the SWCNs as a function of diameter of nanotubes at 298 K, 1.0 g cm⁻³.

thermal conductivity. A high anisotropy in thermal transport properties results in that the thermal conductivity in the axial direction (*x* direction) is obviously larger than that in the channel perpendicular (radial) direction (*y* direction, *z* direction). It is interesting that the radial thermal conductivity changes with the diameter of SWCNs in different way from the axial, which decreases smoothly as the diameter of SWCN decreases, and the smaller the diameter, the more evident the difference of thermal conductivity in the axial and radial directions. The components will tend to be the same and approaching to the bulk when the SWCN size gets larger.

The variation of the components of shear viscosity of the confined water along with the diameters of SWCNs is plotted in Fig. 3. The shear viscosity is a tensor quantity with six components, $\eta_{xy}, \eta_{xz}, \eta_{yx}, \eta_{yz}, \eta_{zx}, \eta_{zy}$ (in double subscripts, the first denotes the direction of velocity, and the second denotes the direction of displacement). Both the viscosity and the thermal conductivity are collective properties of the whole sample rather than that of individual molecules, so it cannot be calculated with the same accuracy as the diffusion coefficients. For a homogeneous fluid, the six components of the shear viscosity should all be equal and so the statistical error can be reduced by averaging over the six components. In SWCNs, owing to the confinement in *y* direction or *z* direction, which hinders the glide of molecular layers required in a shearing flow, so the components, $\eta_{xy}, \eta_{xz}, \eta_{yz}, \eta_{zy}$, in the nanotubes are almost zero. But the components η_{yx} and η_{zx} increase obviously as the diameter of SWCN decreases. In particular, the viscosity dramatically increases in very narrow tubes or pores. In fact, in very-small-size pores, the components $\eta_{xy}, \eta_{xz}, \eta_{yz}, \eta_{zy}$ do not make sense, as the space is confined in *y* direction or *z* direction by the dimensional restriction, the displacement of molecules in confined direction is very little and the molecules hardly move. The viscosity components η_{yx} and η_{zx} are the only sensible definition in such a case with *y* direction or *z* direction confined, because there are obvious displacements of molecules in the axial direction and shearing flow of water molecules. In this work, two of these components, η_{yx} and η_{zx} , were averaged to describe the viscosity of the fluids inside the SWCNs and drawn by the solid lines in

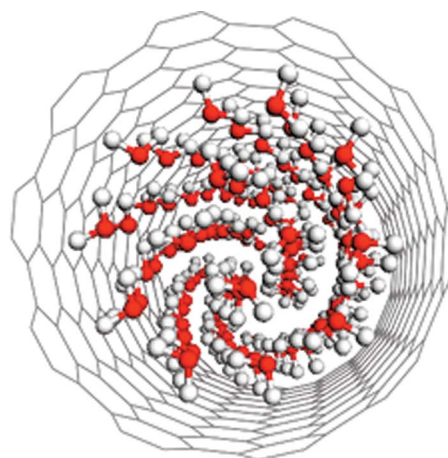


FIG. 4. (Color) A snapshot of the distribution of water molecules confined in (10, 10) SWCN at 298 K, 1.0 g cm⁻³. The water molecules ordered in helix are clearly observable.

Fig. 3. The averaged viscosity of η_{yx} and η_{zx} in SWCNs is larger than that of the bulk, and it increases as the diameter of SWCN decreases. Particularly, the viscosity sharply increases in very narrow pores. Although the viscosity and thermal conductivity increases sharply with diameter of SWCN decreasing, by contrast, the diffusivity decreases slowly. It is originated that the diffusive motion depends only on fluidity to individual molecular movement, not glide of an entire layer or heat transfer of whole sample. This demonstrates that the nature of transport properties in nanotubes is quite different from the bulk fluids, and three aspects of transport property, diffusivity, thermal conductivity, and viscosity, profoundly behave differently.

As reported in Nature magazine,²⁶ the *n*-gonal (*n*=4–6) ice nanotube formed inside the (14, 14), (15, 15), and (16, 16) SWCNs at high pressure (50 MPa) and lower temperature (240 K). But in our simulations, at 298 K and 1.0 g cm⁻³ in (10, 10) SWCN, as shown in Fig. 4, the water molecules ordered in helix inside (10, 10) SWCN, and long-range order in the axial direction was observed also. We considered that the tetrahedron structure of water molecules in O–H bonding and hydrogen bonding, and the strong water molecule to SWCN wall interactions that resulted from the attraction of the water molecules with the π electrons along the C–C bond directions in the SWCNs,³⁰ and spatial effect of SWCN, make helix forming of confined water molecules inside the SWCNs possible and necessary; further investigation by means of quantum mechanics calculations is still underway.

In summary, the transport properties, including the diffusivity, the thermal conductivity, and the shear viscosity, of water confined in SWCNs have been studied with different diameters in this work. The diameter of SWCN makes an important impact on transport properties and molecular distribution of water. A distinct characteristic is that the axial thermal conductivity and viscosity in nanotubes is much higher than that of the bulk, and they increase sharply as the diameter of SWCN decreases, which is in clear contrast to the diffusivity. The diffusivity in SWCNs is much lower than that of the bulk, and it ever decreases as the diameter of SWCN decreases, which is similar to the results for the

model nanopores qualitatively. The water molecules ordered in helix inside (10, 10) SWCN, and long-range order in the axial direction was observed also. This demonstrates that the nature of these transport properties and distribution profile of water molecules confined in nanotubes behaves somewhat particularly to a certain extent.

The authors thank Professor Ponder of Washington University for his kind offering of the TINKER package, so that the authors could modify some of the programs and use them in the MD simulations concerning nanopores. This work was financially supported by the National Natural Science Foundation of China (Grant No. 20176048).

*Email address: qiwang@zju.edu.cn

- ¹S. Supple and N. Quirke, *Phys. Rev. Lett.* **90**, 214501 (2003).
- ²R. R. Henriquez, T. Ito, L. Sun, and R. M. Crooks, *Analyst (Cambridge, U.K.)* **129**, 478 (2004).
- ³A. Kalra, G. Hummer, and S. Garde, *J. Phys. Chem. B* **108**, 544 (2004).
- ⁴T. Werder, J. H. Walther, R. L. Jaffe, T. Halicioglu, F. Noca, and P. Koumoutsakos, *Nano Lett.* **1**, 697 (2001).
- ⁵Z. G. Mao and S. B. Sinnott, *J. Phys. Chem. B* **105**, 6916 (2001).
- ⁶Z. G. Mao and S. B. Sinnott, *J. Phys. Chem. B* **104**, 4618 (2000).
- ⁷G. Hummer, J. C. Rasaiah, and J. P. Noworyt, *Nature (London)* **414**, 188 (2001).
- ⁸X. Zhou, C. Q. Li, and M. Iwamoto, *J. Chem. Phys.* **121**, 7996 (2004).
- ⁹L. Maibaum and D. Chandler, *J. Phys. Chem. B* **107**, 1189 (2003).
- ¹⁰M. P. Rossi, H. H. Ye, Y. Gogotsi, S. Babu, P. Ndungu, and J. C. Bradley, *Nano Lett.* **4**, 989 (2004).
- ¹¹G. A. Fernandez, J. Vrabc, and H. Hasse, *Fluid Phase Equilib.* **221**, 157 (2004).
- ¹²Y. C. Liu, Q. Wang, and L. H. Lu, *J. Chem. Phys.* **120**, 10728 (2004).
- ¹³Y. C. Liu, Q. Wang, and L. H. Lu, *Langmuir* **20**, 6921 (2004).
- ¹⁴Y. C. Liu, Q. Wang, and L. H. Lu, *Chem. Phys. Lett.* **381**, 210 (2003).
- ¹⁵Y. C. Liu, Q. Wang, and L. H. Lu, *Chin. J. Chem.* **22**, 238 (2004).
- ¹⁶Y. C. Liu, Q. Wang, and X. F. Li, *J. Chem. Phys.* **122**, 044714 (2005).
- ¹⁷W. L. Jorgensen, *J. Chem. Phys.* **79**, 926 (1983).
- ¹⁸D. P. Cao, X. R. Zhang, J. F. Chen, W. C. Wang, and J. Yun, *J. Phys. Chem. B* **107**, 13286 (2003).
- ¹⁹M. J. Dudek, K. Ramnarayan, and J. W. Ponder, *J. Comput. Chem.* **19**, 548 (1998).
- ²⁰C. Rapaport, *The Art of Molecular Dynamics Simulation* (Cambridge University Press, Cambridge, UK, 1995).
- ²¹C. R. Kamala, K. G. Ayappa, and S. Yashonath, *Phys. Rev. E* **65**, 061202 (2002).
- ²²Z. G. Mao and S. B. Sinnott, *Phys. Rev. Lett.* **89**, 278301 (2002).
- ²³L. Skoulidas, D. M. Ackerman, J. K. Johnson, and D. S. Sholl, *Phys. Rev. Lett.* **89**, 185901 (2002).
- ²⁴D. P. Cao and J. Z. Wu, *Langmuir* **20**, 3759 (2004).
- ²⁵R. B. Bird, W. E. Stewart, and E. N. Lightfoot, *Transport Phenomena*, 2nd ed. (Wiley, New York, 2002).
- ²⁶K. Koga, G. T. Gao, H. Tanaka, and X. C. Zeng, *Nature (London)* **412**, 802 (2001).
- ²⁷G. Jepps, S. K. Bhatia, and D. J. Searles, *Phys. Rev. Lett.* **91**, 126102 (2003).
- ²⁸C. W. Padgett and D. W. Brenner, *Nano Lett.* **4**, 1051 (2004).
- ²⁹S. Shenogin, A. Bodapati, L. Xue, R. Ozisik, and P. Keblinski, *Appl. Phys. Lett.* **85**, 2229 (2004).
- ³⁰X. Fan, E. C. Dickey, P. C. Eklund, K. A. Williams, L. Grigorian, R. Buczko, S. T. Pantelides, and S. J. Pennycook, *Phys. Rev. Lett.* **84**, 4621 (2001).